JOURNAL OF THERMOPHYSICS AND HEAT TRANSFER
Vol. 24, No. 2, April–June 2010

Master Equation Study and Nonequilibrium Chemical Reactions for Hydrogen Molecule

Jae Gang Kim,* Oh Joon Kwon,† and Chul Park‡
Korea Advanced Institute of Science and Technology, Daejeon 305-701, Republic of Korea

DOI: 10.2514/1.45283

The state-to-state cross sections and rates for collisional transitions of rotational and vibrational states were first calculated by using quasi-classical trajectory calculations for $H_2 + H_2$ collisions. Accuracy of these calculations was verified by comparing them with the results of quantum mechanical and other quasi-classical trajectory calculations. A system of master equations was constructed for a total of 348 ro-vibrational states with these rate coefficients. Unlike in existing works, the internal states of the colliding particles were assumed to be distributed under a Boltzmann distribution specified by a nonequilibrium temperature. The nonequilibrium temperature was in turn determined from the ro-vibrational energy contents. From the results of the master equation calculation, the relaxation rate of vibrational and rotational modes, rate of relaxation of number densities, the average ro-vibrational energy transferred during dissociation, the quasi-steady state rate coefficients, and two-temperature rate coefficients were derived. The present results are different from those of Sharma ("Rotational Relaxation of Molecular Hydrogen at Moderate Temperatures," *Journal of Thermophysics and Heat Transfer*, Vol. 8, No. 1, 1994, pp. 35–39) and of Furudate et al. ("Coupled Rotational-Vibrational Relaxation of Molecular Hydrogen at High Temperatures," *Journal of Thermophysics and Heat Transfer*, Vol. 20, No. 3, 2006, pp. 457–464), and agree closer with existing experimental data.

Nomenclature

c	=	dissociated state
E_0	=	threshold energy, erg
E_{tr}	=	relative translational energy, erg
$E(j)$, $E(v)$, $E(v, j)$	=	rotational, vibrational, and ro-vibrational energy, respectively, erg
e_r, e_v, e_{rv}	=	average rotational, vibrational, and ro-vibrational energy, respectively, erg
ε	=	symmetric factor
ε_{rv}	=	ro-vibrational energy loss, erg
j, v	=	rotational and vibrational energy state, respectively
K_f	=	dissociation rate coefficients of quasi-steady state, $\text{cm}^3\ \text{sec}^{-1}$
$K_{f\text{-two}}$	=	dissociation rate coefficients of two-temperature model, $\text{cm}^3\ \text{sec}^{-1}$
K_r	=	recombination rate coefficients of quasi-steady state, $\text{cm}^6\ \text{sec}^{-1}$
$K(c, c; v_1, j_1, v_2, j_2)$	=	state-to-state rate coefficient for $(c, c) \rightarrow (v_1, j_1, v_2, j_2)$, $\text{cm}^9\ \text{sec}^{-1}$
$K(c, v_2', j_2'; v_1, j_1, v_2, j_2)$	=	state-to-state rate coefficient for $(c, v_2', j_2') \rightarrow (v_1, j_1, v_2, j_2)$, $\text{cm}^6\ \text{sec}^{-1}$
$K(v_1, j_1, v_2, j_2; c, c)$	=	state-to-state rate coefficient for $(v_1, j_1, v_2, j_2) \rightarrow (c, c)$, $\text{cm}^3\ \text{sec}^{-1}$
$K(v_1, j_1, v_2, j_2; c, v_2', j_2')$	=	state-to-state rate coefficient for $(v_1, j_1, v_2, j_2) \rightarrow (c, v_2', j_2')$, $\text{cm}^3\ \text{sec}^{-1}$
$K(v_1, j_1, v_2, j_2; v_1', j_1', c)$	=	state-to-state rate coefficient for $(v_1, j_1, v_2, j_2) \rightarrow (v_1', j_1', c)$, $\text{cm}^3\ \text{sec}^{-1}$
$K(v_1, j_1, v_2, j_2; v_1', j_1', v_2', j_2')$	=	state-to-state rate coefficient for $(v_1, j_1, v_2, j_2) \rightarrow (v_1', j_1', v_2', j_2')$, $\text{cm}^3\ \text{sec}^{-1}$
$K(v_1', j_1', v_2', j_2'; v_1, j_1, v_2, j_2;)$	=	state-to-state rate coefficient for $(v_1', j_1', v_2', j_2') \rightarrow (v_1, j_1, v_2, j_2)$, $\text{cm}^3\ \text{sec}^{-1}$
$K(v_1', j_1', v_2', j_2'; c, v_2, j_2)$	=	state-to-state rate coefficient for $(v_1', j_1', v_2', j_2') \rightarrow (c, v_2, j_2)$, $\text{cm}^3\ \text{sec}^{-1}$
k	=	Boltzmann constant, erg/K
μ	=	reduced mass, g
N_{H}	=	number density of dissociated hydrogen atom, cm^{-3}
N_M	=	number density of colliding molecule, cm^{-3}
$N_{v,j}$	=	number density of hydrogen molecule of (v, j) state, cm^{-3}
Q_m	=	molecular partition function
$Q_{v,j}$	=	partition function for (v, j) state and translational temperature
$Q(v, j; T_{\text{rv}})$	=	partition function for (v, j) state and ro-vibrational temperature
ρ_{H}	=	normalized number density of atomic hydrogen
$\rho_{v,j}$	=	normalized number density of molecular hydrogen for (v, j) state
$\sigma(v_1, j_1, v_2, j_2; c, c)$	=	state-to-state cross section for $(v_1, j_1, v_2, j_2) \rightarrow (c, c)$, cm^2

Presented as Paper 1023 at the 47th AIAA Aerospace Sciences Meeting New Horizon and Aerospace Exposition, Orlando, FL, 5–8 January 2009; received 5 May 2009; revision received 17 November 2009; accepted for publication 28 November 2009. Copyright © 2009 by the American Institute of Aeronautics and Astronautics, Inc. All rights reserved. Copies of this paper may be made for personal or internal use, on condition that the copier pay the $10.00 per-copy fee to the Copyright Clearance Center, Inc., 222 Rosewood Drive, Danvers, MA 01923; include the code 0887-8722/10 and $10.00 in correspondence with the CCC.

*Research Assistant, Department of Aerospace Engineering; berlioz0@kaist.ac.kr. Student Member AIAA.

†Professor, Department of Aerospace Engineering; ojkwon@kaist.ac.kr. Senior Member AIAA.

‡Invited Professor, Department of Aerospace Engineering; cpark216@kaist.ac.kr. Fellow AIAA.

$\sigma(v_1, j_1, v_2, j_2; c, v_1', j_2')$ = state-to-state cross section for $(v_1, j_1, v_2, j_2) \rightarrow (c, v_1', j_2')$, cm^2

$\sigma(v_1, j_1, v_2, j_2; v_1', j_1', c)$ = state-to-state cross section for $(v_1, j_1, v_2, j_2) \rightarrow (v_1', j_1', c)$, cm^2

$\sigma(v_1, j_1, v_2, j_2; v_1', j_1', v_2', j_2')$ = state-to-state cross section for $(v_1, j_1, v_2, j_2) \rightarrow (v_1', j_1', v_2', j_2')$, cm^2

T, T_r, T_v, T_{rv} = translational, rotational, vibrational, and ro-vibrational temperature, respectively, K

t = time, sec

t_c = elastic collision time, sec

τ_r, τ_v = rotational and vibrational relaxation time, respectively, sec

Subscripts

Eq = equilibrium state

i, j, l, m = index of ro-vibrational state

1,2 = particle index

I. Introduction

THE atmospheres of outer planets consist mostly of H_2 molecules and a small concentration of He atoms. For future outer planetary missions, it is necessary to analyze the nonequilibrium phenomena of H_2 and He. The relaxation patterns of rotational and vibrational temperatures of H_2 are expected to be different from those of N_2 and O_2. In the case of N_2 and O_2, rotational temperature relaxation is completed faster than vibrational temperature relaxation [1]. For H_2, the energy gaps between the adjacent rotational states are as large as those between vibrational states [2]. Therefore, for H_2, a strong coupling may occur among the rotational, vibrational, and translational modes during collisions (RVT transitions). The RVT transitions for the $H_2 + H$ and $H_2 + He$ collisions were investigated in a previous study [3]. For $H_2 + H_2$ collisions, Sharma [4] derived the rotational relaxation time for temperatures up to 5000 K by solving the master equation, where a quasi-classical trajectory (QCT) method by Schwenke [5] was employed to obtain the state-to-state rate coefficients. Furudate et al. [6] extended this rotational relaxation model to 50,000 K. The state-to-state rates in their work were obtained by using a similar QCT method developed earlier by Fujita and Abe [7].

However, uncertainties exist in those previous studies for $H_2 + H_2$ collisions [4,6]. In those studies, the state-to-state rate coefficients were obtained under an implicit assumption that the internal states of colliding particles H_2 are in Boltzmann distribution specified by the translational temperature. The rotational relaxation times calculated by Sharma [4] deviated severely from the measured values at around 1500 K. In the work of Furudate et al. [6] an arbitrarily chosen multiplication factor was introduced to bring the calculated rates to approximately the same values as Sharma's rates. These procedures introduce uncertainties in the state-to-state rate values used by those investigators [4,6].

There are a total of 348 ro-vibrational states, and therefore, that many differential equations in the master equation set describing ro-vibrational relaxation. There are $348 \times 347/2 + 348 = 60,726$ rate coefficients. Each of these 60,726 transitions affects the ro-vibrational states of both target and colliding particles. A faithful description of these phenomena will require prohibitively large computing resources. Both Sharma [4] and Furudate et al. [6] simplified the problem by assuming that the internal states of colliding particles are populated in a Boltzmann distribution characterized by the translational temperature. The changes in the internal states of the colliding particles were not accounted for in the master equation calculations.

To overcome these shortcomings in the previous investigations ([4,6]) a different approach was made in the present study. Unlike in the previous studies ([4,6]) the internal states of the colliding H_2 were assumed to be populated according to an arbitrary nonequilibrium temperature. This nonequilibrium temperature was evaluated at every time step from the local ro-vibrational state distribution. The sampling for the QCT calculations was carried out with this constraint on the internal state distribution for the colliding particles. This procedure introduced ro-vibrational transition rate coefficients that are a function of both translational and ro-vibrational temperatures. Using these new rate coefficients, the counting over the internal states of the colliding particles was eliminated completely. This approach reduced the computing resources greatly. Yet, the transitions in both colliding and target molecules were fully accounted for on the average.

From the results of the mater equation calculation, the relaxation rate of vibrational and rotational modes, rate of relaxation of number densities, the average ro-vibrational energy transferred during dissociation, the quasi-steady state (QSS) rate coefficients, and two-temperature rate coefficients were derived.

II. Method of Analysis

A. Formulation of Master Equation

The number density of the molecules N_{v_1,j_1} for a ro-vibrational state (v_1, j_1) is affected by the incoming and outgoing rates of transitions. An incoming rate is the rate of individual transition from an initial ro-vibrational state (v_1', j_1') or a free state c to a final ro-vibrational state (v_1, j_1) by a collision with a colliding particle $H_2(v_2', j_2')$ or a free state c. When the incoming rate is a bound–bound transition, the rate of transition is given by $K(v_1', j_1', v_2', j_2'; v_1, j_1, v_2, j_2)N_{v_1',j_1'}N_{v_2',j_2'}$ and $K(v_1', j_1', c; v_1, j_1, v_2, j_2)N_{v_1',j_1'}N_H^2$. When the incoming rate is free-bound transition, it is given by $K(c, v_2', j_2'; v_1, j_1, v_2, j_2)N_H^2 N_{v_2',j_2'}$ and $K(c, c; v_1, j_1, v_2, j_2)N_H^4$. For the reverse process of outgoing rate, the rate for bound–bound transition is $K(v_1, j_1, v_2, j_2; v_1', j_1', v_2', j_2')N_{v_1,j_1}N_{v_2,j_2}$ and $K(v_1, j_1, v_2, j_2; v_1', j_1', c)N_{v_1,j_1}N_{v_2,j_2}$, and the bound-free transition is $K(v_1, j_1, v_2, j_2; c, v_2', j_2')N_{v_1,j_1}N_{v_2,j_2}$ and $K(v_1, j_1, v_2, j_2; c, c)N_{v_1,j_1}N_{v_2,j_2}$. The time rate of change of N_{v_1,j_1} is the difference between the sum of all incoming rates and the sum of all outgoing rates

$$\begin{aligned}\frac{\partial N_{v_1,j_1}}{\partial t} = &\sum_{j,\ell,m(\ell\le m)} \varepsilon_{ij\ell m}[-K(v_1, j_1, v_2, j_2; v_1', j_1', v_2', j_2')N_{v_1,j_1}N_{v_2,j_2} \\ &+ K(v_1', j_1', v_2', j_2'; v_1, j_1, v_2, j_2)N_{v_1',j_1'}N_{v_2',j_2'}] \\ &+ \sum_{j,\ell} \varepsilon_{ij\ell}[-K(v_1, j_1, v_2, j_2; v_1', j_1', c)N_{v_1,j_1}N_{v_2,j_2} \\ &+ K(v_1', j_1', c; v_1, j_1, v_2, j_2)N_{v_1',j_1'}N_H^2] \\ &+ \sum_{j,m} \varepsilon_{ijm}[-K(v_1, j_1, v_2, j_2; c, v_2', j_2')N_{v_1,j_1}N_{v_2,j_2} \\ &+ K(c, v_2', j_2'; v_1, j_1, v_2, j_2)N_H^2 N_{v_2',j_2'}] \\ &+ \sum_{j} \varepsilon_{ij}[-K(v_1, j_1, v_2, j_2; c, c)N_{v_1,j_1}N_{v_2,j_2} \\ &+ K(c, c; v_1, j_1, v_2, j_2)N_H^4] \end{aligned} \quad (1)$$

where the indices i, j, ℓ, and m represent the ro-vibrational state of (v_1, j_1), (v_2, j_2), (v_1', j_1'), and (v_2', j_2'), respectively. The symmetric factor ε is

$$\varepsilon_{ij\ell m} = [1 + \delta_{ij}(1 - \delta_{\ell i})(1 - \delta_{mi})][1 - \delta_{\ell i}(1 - \delta_{ij})][1 - \delta_{mi}(1 - \delta_{ij})] \quad (2)$$

$$\varepsilon_{ij\ell} = [1 + \delta_{ij}(1 - \delta_{\ell i})][1 - \delta_{\ell i}(1 - \delta_{ij})] \quad (3)$$

$$\varepsilon_{ijm} = [1 + \delta_{ij}(1 - \delta_{mi})][1 - \delta_{mi}(1 - \delta_{ij})] \quad (4)$$

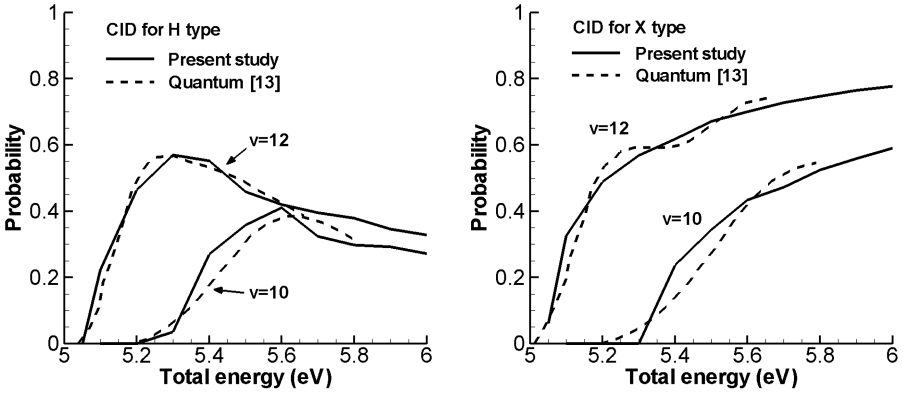

a) b)

Fig. 1 Comparison of the CID probabilities of dissociation reactions for H- and X-type collisions between the present study and the quantum mechanical calculations by Bartolomei et al. [13]: a) $H_2(v = 10, 12, j = 0) + H_2(0, 0) \rightarrow$ CID for H-type collisions, and b) $H_2(v = 10, 12, j = 0) + H_2(0, 0) \rightarrow$ CID for X-type collisions.

$$\varepsilon_{ij} = [1 + \delta_{ij}] \tag{5}$$

Also, the time rate of change of dissociated H atom number density can be expressed as

$$\begin{aligned}\frac{\partial N_{\mathrm{H}}}{\partial t} = &\sum_{i,j,m} 2[K(v_1, j_1, v_2, j_2; c, v_2', j_2')N_{v_1,j_1}N_{v_2,j_2} \\ &- K(c, v_2', j_2'; v_1, j_1, v_2, j_2)N_{v_1',j_1'}N_{\mathrm{H}}^2] \\ &+ \sum_{i,j} 2[K(v_1, j_1, v_2, j_2; c, c)N_{v_1,j_1}N_{v_2,j_2} \\ &- K(c, c; v_1, j_1, v_2, j_2)N_{\mathrm{H}}^4]\end{aligned} \tag{6}$$

However, the evaluation of the master Eqs. (1) and (6) is practically impossible. Evaluating the 60,726 rate coefficients in Eqs. (1) and (6) requires prohibitively large computing resources. The summation in Eqs. (1) and (6) will also require large computing resources. Thus, to evaluate the rates of rotational and vibrational relaxation and of number density, it is necessary to modify the master equation such that the calculation can be performed with a reasonable computational cost.

The results by Furudate et al. [6] show that the internal state distribution in the ro-vibrational nonequilibrium state is nearly Boltzmann characterized by a ro-vibrational temperature [6]. Therefore, the number density of colliding particles can be expressed approximately as

$$N(v_2, j_2) = N_M \frac{Q(v_2, j_2, T_{\mathrm{rv}})}{\sum_{v,j} Q(v_2, j_2, T_{\mathrm{rv}})} \tag{7}$$

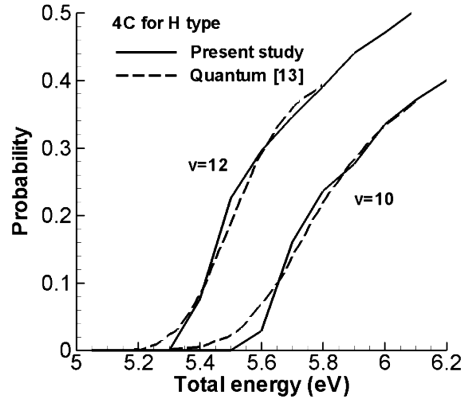

Fig. 2 Comparison of the 4C probability of exchange reaction for H-type collision between the present study and the quantum mechanical calculations by Bartolomei et al. [13].

The principle of the detailed balancing relation between the forward and backward rates is invoked under an equilibrium, which leads to

$$\begin{aligned}&K(v_1, j_1, v_2, j_2; v_1', j_1', v_2', j_2')N_{v_1,j_1;\mathrm{Eq}}N_{v_2,j_2;\mathrm{Eq}} \\ &\quad = K(v_1', j_1', v_2', j_2'; v_1, j_1, v_2, j_2)N_{v_1',j_1';\mathrm{Eq}}N_{v_2',j_2';\mathrm{Eq}}\end{aligned} \tag{8}$$

$$\begin{aligned}&K(v_1, j_1, v_2, j_2; v_1', j_1', c)N_{v_1,j_1;\mathrm{Eq}}N_{v_2,j_2;\mathrm{Eq}} \\ &\quad = K(v_1', j_1', c; v_1, j_1, v_2, j_2)N_{v_1',j_1';\mathrm{Eq}}N_{\mathrm{H;Eq}}^2\end{aligned} \tag{9}$$

$$\begin{aligned}&K(v_1, j_1, v_2, j_2; c, v_2', j_2')N_{v_1,j_1;\mathrm{Eq}}N_{v_2,j_2;\mathrm{Eq}} \\ &\quad = K(c, v_2', j_2'; v_1, j_1, v_2, j_2)N_{\mathrm{H;Eq}}^2N_{v_2',j_2';\mathrm{Eq}}\end{aligned} \tag{10}$$

$$K(v_1, j_1, v_2, j_2; c, c)N_{v_1,j_1;\mathrm{Eq}}N_{v_2,j_2;\mathrm{Eq}} = K(c, c; v_1, j_1, v_2, j_2)N_{\mathrm{H;Eq}}^4 \tag{11}$$

The normalized number density ρ is defined as the ratio of the nonequilibrium number density to the equilibrium number density, and for a specific (v, j) state, can be written as $\rho_{v,j} = N_{v,j}/N_{v,j;\mathrm{Eq}}$. The normalized number density for H is $\rho_{\mathrm{H}} = N_{\mathrm{H}}/N_{\mathrm{H;Eq}}$. By using Eqs. (7–11) and the normalized number densities, the master Eqs. (1) and (6) can be rewritten in the following form after some manipulations:

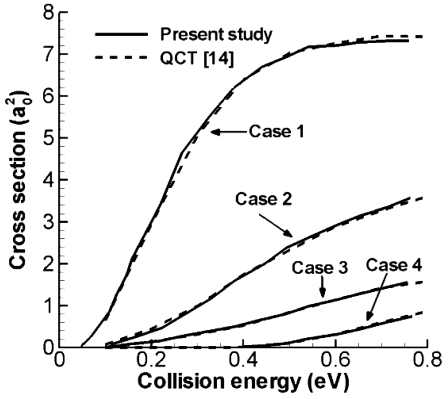

Fig. 3 Comparison of the state-to-state cross sections between the present study and the QCT calculations by Mandy and Pogrebnya [14], where case 1 for $H_2(0, 0) + H_2(1, 0) \rightarrow H_2(0, 0) + H_2(1, 2)$, case 2 for $H_2(0, 2) + H_2(1, 2) \rightarrow H_2(0, 2) + H_2(1, 4)$, case 3 for $H_2(0, 2) + H_2(1, 2) \rightarrow H_2(0, 4) + H_2(1, 2)$, and case 4 for $H_2(0, 4) + H_2(1, 0) \rightarrow H_2(0, 6) + H_2(1, 2)$.

$$\frac{\partial \rho_{v_1,j_1}}{\partial t} = \sum_{v_1'=0}^{\max v_1'} \sum_{j_1'=0}^{\max j_1'} N_M K(v_1, j_1; v_1', j_1'; T_{\mathrm{rv}})[\rho_{v_1',j_1'} - \rho_{v_1,j_1}] + N_M K(v_1, j_1; c; T_{\mathrm{rv}})[\rho_{\mathrm{H}}^2 - \rho_{v_1,j_1}] \quad (12)$$

$$\frac{\partial \rho_{\mathrm{H}}}{\partial t} = 2 \sum_{v_1=0}^{\max v_1} \sum_{j_1=0}^{\max j_1} \frac{N_{v_1,j_1;\mathrm{Eq}} N_M}{N_{\mathrm{H;Eq}}} K(v_1, j_1; c; T_{\mathrm{rv}})[\rho_{v_1,j_1} - \rho_{\mathrm{H}}^2] \quad (13)$$

where the state-to-state rate coefficients are

$$K(v_1, j_1; v_1', j_1'; T_{\mathrm{rv}}) = \left(\frac{8kT}{\pi\mu}\right)^{1/2} \int_{E_0}^{\infty} \frac{E_{\mathrm{tr}}}{kT} \exp\left(-\frac{E_{\mathrm{tr}}}{kT}\right) \mathrm{d}\left(-\frac{E_{\mathrm{tr}}}{kT}\right) \left[\int_{v_2,j_2} \int_{v_2',j_2'} \frac{Q(v_2, j_2, T_{\mathrm{rv}})}{\sum_{v_2,j_2} Q(v_2, j_2, T_{\mathrm{rv}})} \sigma(v_1, j_1, v_2, j_2; v_1', j_1', v_2', j_2'; E_{\mathrm{tr}}) \, \mathrm{d}v_2' \, \mathrm{d}j_2' \, \mathrm{d}v_2 \, \mathrm{d}j_2 + \int_{v_2,j_2} \frac{Q(v_2, j_2, T_{\mathrm{rv}})}{\sum_{v_2,j_2} Q(v_2, j_2, T_{\mathrm{rv}})} \sigma(v_1, j_1, v_2, j_2; v_1', j_1', c; E_{\mathrm{tr}}) \, \mathrm{d}v_2 \, \mathrm{d}j_2 \right] \quad (14)$$

$$K(v_1, j_1; c; T_{\mathrm{rv}}) = \left(\frac{8kT}{\pi\mu}\right)^{1/2} \int_{E_0}^{\infty} \frac{E_{\mathrm{tr}}}{kT} \exp\left(-\frac{E_{\mathrm{tr}}}{kT}\right) \mathrm{d}\left(-\frac{E_{\mathrm{tr}}}{kT}\right) \left[\int_{v_2,j_2} \int_{v_2',j_2'} \frac{Q(v_2, j_2, T_{\mathrm{rv}})}{\sum_{v_2,j_2} Q(v_2, j_2, T_{\mathrm{rv}})} \sigma(v_1, j_1, v_2, j_2; c, v_2', j_2'; E_{\mathrm{tr}}) \, \mathrm{d}v_2' \, \mathrm{d}j_2' \, \mathrm{d}v_2 \, \mathrm{d}j_2 + \int_{v_2,j_2} \frac{Q(v_2, j_2, T_{\mathrm{rv}})}{\sum_{v_2,j_2} Q(v_2, j_2, T_{\mathrm{rv}})} \sigma(v_1, j_1, v_2, j_2; c, c; E_{\mathrm{tr}}) \, \mathrm{d}v_2 \, \mathrm{d}j_2 \right] \quad (15)$$

As seen in Eqs. (12) and (13), the presence of H was not accounted for in the master equation. This was done so to limit the present inquiry only to the effect of H_2 collisions.

Equation (13) and a total of 348 equations in the form of Eq. (12) are to be integrated numerically to obtain $\rho_{v,j}$ and ρ_{H} as a function of time. For solving these 349 stiff equations, an implicit time integration algorithm [8] was used in the present study.

B. State-to-State Rate Coefficients

In the present study, the state-to-state rate coefficients in Eqs. (14) and (15) were calculated from the state-to-state cross sections evaluated by the QCT method. In these calculations, the Schwenke potential energy surface (PES) [5] was used for the interaction of $H_2 + H_2$ collisions. All trajectories were initiated by the internal energies that correspond precisely to each of the 348 (v, j) states of H_2. To determine the initial coordinates and the conjugated momenta of H_2 given by the exact Schwenke PES ([5]), a fast Fourier transform method proposed by Eaker [9] was used with some modifications. In the present QCT calculations, stratified sampling was adopted to obtain the impact parameter, and all other parameters were Monte Carlo-selected. The final rotational and vibrational energy levels were quantized by the Wentzel, Kramers, and Brillouin approximation method [10]. Also, the quasi-bound states were determined from the effective potential method proposed by Kuntz, [11] and the collisions were calculated in a classical manner. A total of 3000 trajectories were calculated per impact parameter at the batch size of 0.1 Å (A). To ensure the convergence of the cross sections, the calculations were repeated until all collisions became elastic. Reactive and nonreactive trajectories were treated separately in the calculations of the cross sections. The nonreactive trajectories were counted as described by Mandy et al. [12], whereas the reactive trajectories were counted twice: the first as ortho-state with a weighting of 3/4 due to nuclear spin, and the second as para-state with a weighting of 1/4. Further details about the QCT calculations can be found in other literatures [10,11].

To validate the QCT method used in the present study, state-to-state probabilities and cross sections were compared with those calculated by a quantum mechanical method [13] and other QCT methods [14]. Both quantum mechanical and QCT calculations were based on the Boothroyd, Martin, Keogh, and Peterson (BMKP) PES [15]. To validate the QCT method, the BMKP PES was also used in the present study for validation cases.

In Figs. 1 and 2, the probabilities of collision induced dissociation (CID) and exchange reaction (4C) of the present study are compared with the results of quantum mechanical calculations [13] for $H_2(v = 10, 12, j = 0) + H_2(0, 0)$ collisions. A first batch of QCT calculations was carried out by using dynamical constraints, similar to those of the quantum mechanical calculations, by forcing the motion to occur on the plane of the initial H and X types. For H-type collisions, reactant H_2 was forced to vibrate along the parallel direction perpendicular to the relative velocity vector without rotation and to collide with zero impact parameter. For X-type collisions, reactant H_2 vibrates along the orthogonal direction perpendicular to the relative velocity vector without rotation. The results show that for the CID reaction, the probabilities of the present study agree well with those of the quantum mechanical calculations, except the threshold energies. In the threshold energies, the QCT results are sharper than the quantum mechanical results. These effects have already been noted in other CID studies and named as quantum tails [12]. However, this quantum tail is not so significant in calculating the state-to-state rate coefficients. Similar results were also obtained

Table 1 Initial conditions for the modified master equation study of molecular hydrogen collisions in heating and cooling environments

	Heating environment			Cooling environment		
	$T_r = T_v$, K	T, K	Number density, cm^{-3}	$T_r = T_v$, K	T, K	Number density, cm^{-3})
Case 1	2000 K	4000 K	1.0×10^{18}	10,000 K	2000 K	1.0×10^{18}
Case 2	2000 K	6000 K	1.0×10^{18}	10,000 K	4000 K	1.0×10^{18}
Case 3	2000 K	8000 K	1.0×10^{18}	10,000 K	6000 K	1.0×10^{18}
Case 4	2000 K	10,000 K	1.0×10^{18}	-	-	-
Case 5	2000 K	20,000 K	1.0×10^{18}	-	-	-
Case 6	2000 K	30,000 K	1.0×10^{18}	-	-	-
Case 7	2000 K	10,000 K	1.0×10^{19}	-	-	-

for the 4C reactions. It is shown that except for the threshold energies, the probabilities for the 4C reactions of the present study agree well with those of the quantum mechanical calculations.

In Fig. 3, the state-to-state cross sections of the present study are compared with the results of the QCT calculations by Mandy and Pogrebnya [14] for the interaction of $H_2(0, j = 0, 2, 4) + H_2(1, j = 0, 2)$. The figure shows that the two results are similar to each other, demonstrating that the QCT method of the present study is correct.

III. Master Equation Study

A. Rotational and Vibrational Temperature Relaxations

The normalized number density densities $\rho_{v,j}$ for all 348 ro-vibrational states and ρ_H were calculated for heating and cooling environments by the master equation of Eqs. (12) and (13). The initial conditions of seven heating and three cooling cases for the $H_2 + H_2$ collisions are tabulated in Table 1. In these calculations, it was assumed that rotational and vibrational excitations and chemical reactions occur at an isothermal condition.

The energy-equivalent rotational, vibrational, and ro-vibrational temperatures that were used in the master equation study can be determined from the average rotational energy e_r, vibrational energy e_v, and ro-vibrational energy e_{rv}, respectively. These average energies are defined as

$$e_r = \frac{\sum_v \sum_j E(j) N_{v,j;\mathrm{Eq}} \rho_{v,j}}{\sum_v \sum_j N_{v,j;\mathrm{Eq}} \rho_{v,j}} \tag{16}$$

$$e_v = \frac{\sum_v \sum_j E(v) N_{v,j;\mathrm{Eq}} \rho_{v,j}}{\sum_v \sum_j N_{v,j;\mathrm{Eq}} \rho_{v,j}} \tag{17}$$

$$e_{rv} = \frac{\sum_v \sum_j E(v,j) N_{v,j;\mathrm{Eq}} \rho_{v,j}}{\sum_v \sum_j N_{v,j;\mathrm{Eq}} \rho_{v,j}} \tag{18}$$

In Fig. 4, the theoretical rotational relaxation parameter $p\tau_r$ for the $H_2 + H_2$ collisions calculated by the present study is compared with the experimental results [16] and other theoretical predictions by Sharma [4] and Furudate et al. [6]. The rotational relaxation is determined by the Landau–Teller equation ([17]) as

$$\frac{\partial e_r}{\partial t} = \frac{e_{r;\mathrm{Eq}}(T) - e_r(T_r)}{\tau_r} \tag{19}$$

By multiplying pressure, one obtains the characteristic rotational relaxation parameter $p\tau_r$. The figure shows that at 1000 K, the rotational relaxation parameter of the present study agrees well with the experimental value of Lensch and Gronig [16]. Up to 30,000 K, the relaxation parameter of the present study has the similar value with the uncorrected case of Furudate et al. [6], where the difference of corrected and uncorrected case is the existence of correction factor $(T/1000)^{-1/2}$, which is the multiplication factor to bring the rates to approximately the same values as the state-to-state rate transition of Sharma. However, a large discrepancy in the rotational relaxation parameter is observed between the present study and Sharma's results [4].

In Fig. 5, the theoretical vibrational relaxation parameter $p\tau_v$ calculated by the present study is compared with the experimental results [18] and other theoretical calculations by Furudate et al. [6]. The experimental vibrational relaxation parameter of gaseous H_2 was obtained by Dove and Teitelbaum [18] using a laser Schlieren technique by measuring the relaxation time of incident shock waves at temperatures between 1350 and 3000 K. In the present study, in a way similar to the rotational relaxation, the vibrational relaxation is determined as

$$\frac{\partial e_v}{\partial t} = \frac{e_{v;\mathrm{Eq}}(T) - e_v(T_v)}{\tau_v} \tag{20}$$

The figure shows that the present theoretical relaxation parameter compares well with the measurement, [18] except for the 2000 K case. For the 2000 K case a difference occurs, because at this high temperature, the number of QCT trials is not sufficient to obtain the very small values of the rate coefficient. The present results are in better agreement with the experimental data than the results by Furudate et al. [6].

In Fig. 6, the rotational and vibrational temperatures, the number density of dissociated H evaluated by the present master equation of Eqs. (12) and (13), and the population distribution of H_2 are compared with the results of the previous master equation used in the works of Sharma [4] and Furudate et al. [6] for the heating environment. In Fig. 6a, the rotational and vibrational relaxations of the present study occur faster, but the starting points of the relaxations are delayed further than the previous master equation for both cases 4 and 5. This is because the internal energy of the colliding H_2 in the present study is smaller than in the previous studies [4,6]. In the present study, it is the nonBoltzmann value evaluated at each time step, whereas in the previous studies, the internal energy of the colliding H_2 was a Boltzmann value corresponding to the translational temperature that is higher than the presently calculated nonequilibrium temperature. In Fig. 6a, The QSS period is also observed in the results of both present and previous master equations. However, for the present master equation, the range of the rotational and vibrational temperatures where the QSS phenomenon is observed is different from that of the previous master equation. For case 4, the discrepancy of the

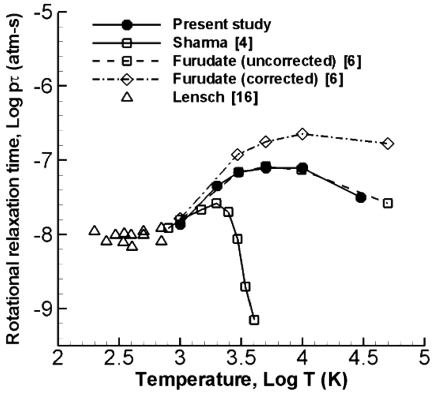

Fig. 4 Comparison of the rotational relaxation parameter between the present study and the theoretical predictions by Sharma [4], Furudate et al. [6], and the experiment by Lensch and Gronig [16].

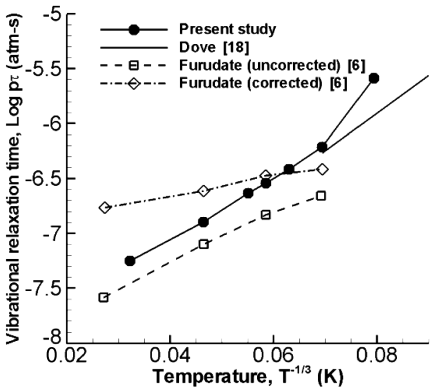

Fig. 5 Comparison of the vibrational relaxation parameter between the present study and the theoretical predictions by Furudate et al. [6] and the experiment by Dove and Teitelbaum [18].

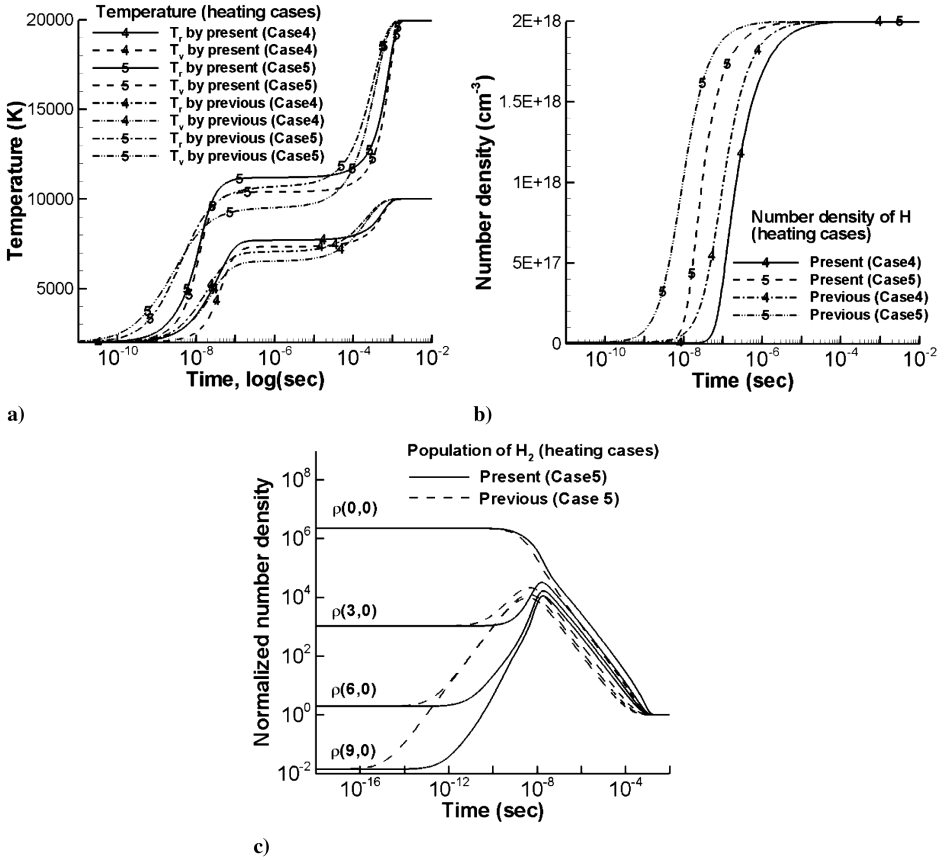

Fig. 6 Comparison of the rotational and vibrational temperatures and the number density of dissociated H atom between the modified master equation and the previous master equation [4,6] for the heating environment: a) rotational and vibrational temperatures for cases 4 and 5, b) number density for cases 4 and 5, and c) population distribution for case 5.

rotational and vibrational temperatures between the present and previous master equations is about 800 K, and for case 5, the discrepancy is about 1000 K. For nonequilibrium chemical reactions, the rotational and vibrational temperatures of the QSS period are important, because the number density rapidly increases during this QSS period, and the reaction rate coefficients, which represent the nonequilibrium chemical reactions, are affected by the rotational and vibrational temperatures of the QSS period. In Fig. 6b, the difference in incubation time due to the difference in the rotational and vibrational temperatures during the QSS period exist between the present and previous master equations. The incubation time of the number density relaxation is longer and the relaxation curve is steeper than those of the previous master equation. In Fig. 6c, the normalized number density of the present master equation for $v = 0, 3, 6$, and 9 is compared with that of the previous master equation. It is shown that a discernible difference of the population distribution of H_2 exists between the present and previous master equations. For $\rho(0, 0)$, the population of the present master equation is similar to the previous master equation. However, for the normalized number density at high vibrational levels of $v = 3$, 6, and 9, the populations of the present master equation are further delayed than those of the previous master equation.

In Fig. 7, the rotational and vibrational temperatures, the number density of the recombined H_2 evaluated by the present master equation of Eqs. (12) and (13), and the population distribution of H_2 are compared with the results of the previous master equation used in the works of Sharma [4] and Furudate et al. [6] for cooling environments. Discernible differences exist in the relaxation patterns of the rotational and vibrational temperatures and the number density. The rotational and vibrational temperatures of the present master equation slightly increase during the period where the number density of the recombined H_2 is rapidly increased. This is because in this region, the number density of the high-energy level molecules is increased due to recombination, and this recombination occurs in a much faster rate than the rotational and vibrational relaxations. These phenomena were also observed in experiments [19,20] and in a theoretical study [21]. However, the temperature-rise phenomena calculated by the previous master equation is much larger than the temperature-rise calculated by the present master equation. Comparison of the population distributions of the normalized number density for $v = 0, 3, 6, 9$, and 12 shows discernible difference between the present and previous master equations. At high vibrational levels of $v = 6$, 9, and 12, the populations of the present master equation are much lower than those of the previous master equation. The difference of the population distribution also induces different temperature-rise phenomena.

In Fig. 8, the rotational and vibrational relaxations evaluated by the master equation of Eqs. (12) and (13) are compared for various temperatures in heating environments. A QSS period is observed in all cases except case 1. During this QSS period, the rotational and vibrational temperatures are almost constant, and the number density of dissociated H rapidly increases. For the temperature relaxation, rotational relaxation occurs faster than vibrational relaxation for cases 1 and 2. However, for cases 3–6, the rotational and vibrational relaxation patterns are similar. These results show that for temperatures above 10,000 K, the rotational and vibrational relaxations have almost similar patterns.

In Fig. 9, the rotational and vibrational relaxations evaluated by the master equation of Eqs. (12) and (13) are compared for various temperatures in cooling environments. The temperature-rise phenomena for the $H_2 + H_2$ collisions are observed in all cases.

When a gas molecule dissociates due to collisions with other particles, the ro-vibrational energy contents of the gas are reduced. This dissociation typically occurs at upper energy states. The rate of ro-vibrational energy loss due to the transition from a (v, j) state is $K(v, j; c; T_{\mathrm{rv}})E(v, j)N_{v,j}N_M$. In the reverse process of recombination, this ro-vibrational energy is added to the (v, j) state. The average ro-vibrational energy loss $\varepsilon_{\mathrm{rv}}$ can be defined as

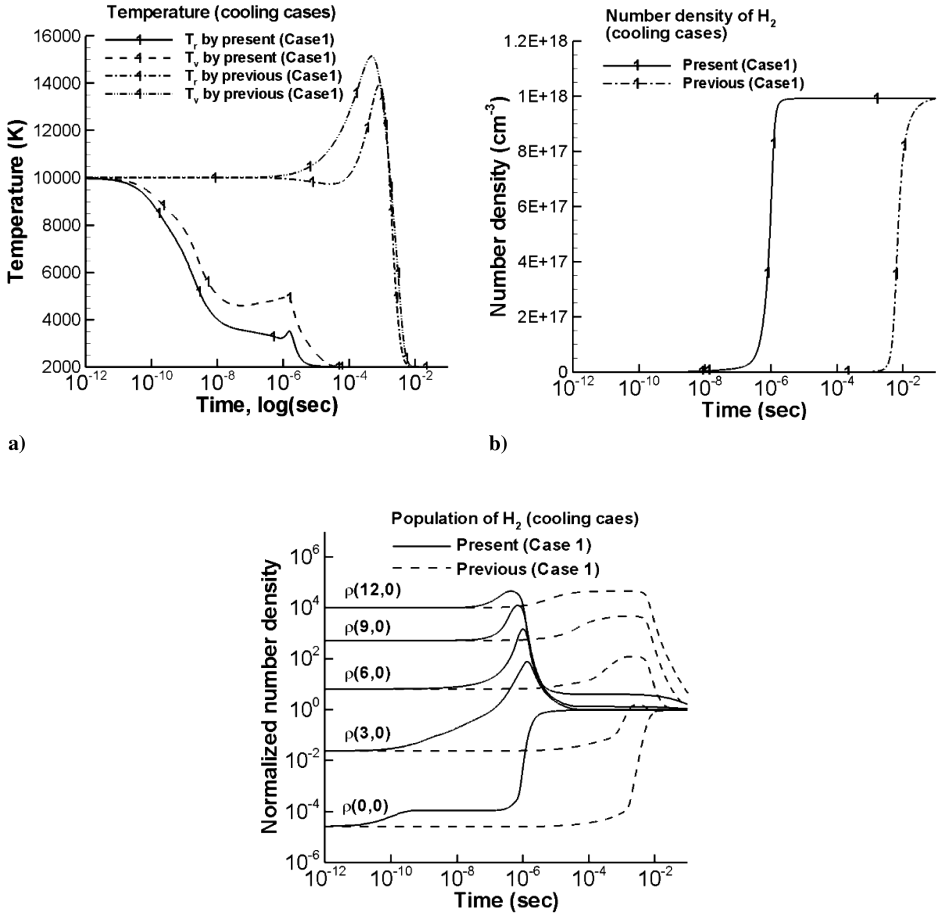

Fig. 7 Comparison of the rotational and vibrational temperatures and the number density of recombinated H_2 molecule between the modified master equation and the previous master equation [4,6] for the cooling environment of case 1: a) rotational and vibrational temperatures, b) number density, and c) population distribution.

$$-\varepsilon_{\mathrm{rv}}\frac{\partial N_{\mathrm{H_2}}}{\partial t} = N_M \sum_{v=0}^{\max v}\sum_{j=0}^{\max j} E(v,j)K(v,j;c;T_{\mathrm{rv}})N_{v,j} - N_M\frac{N_{\mathrm{H}}^2}{4}\sum_{v=0}^{\max v}\sum_{j=0}^{\max j} E(v,j)K(c;v,j;T_{\mathrm{rv}}) \tag{21}$$

Using the detailed balancing relation and the rate of change of density of the atom in Eq. (13), the average ro-vibrational energy loss $\varepsilon_{\mathrm{rv}}$ can be expressed as

$$\varepsilon_{\mathrm{rv}} = \frac{\sum_{v=0}^{\max v}\sum_{j=0}^{\max j} E(v,j)K(v,j;c;T_{\mathrm{rv}})\frac{Q_{v,j}}{Q_m}[\rho_{v,j}-\rho_{\mathrm{H}}^2]}{\sum_{v=0}^{\max v}\sum_{j=0}^{\max j} K(v,j;c;T_{\mathrm{rv}})\frac{Q_{v,j}}{Q_m}[\rho_{v,j}-\rho_{\mathrm{H}}^2]} \tag{22}$$

In Fig. 10, the average ro-vibrational energy loss due to dissociation is compared with the results of Furudate et al. [6] in terms of the translational temperature. The average ro-vibrational energy loss during the QSS period in the present study rises with temperature. Energy loss due to dissociation energy is about 0.24 at a temperature of 5000 K. The present results are very different from those of Furudate et al. at temperatures below 20,000 K; the energy

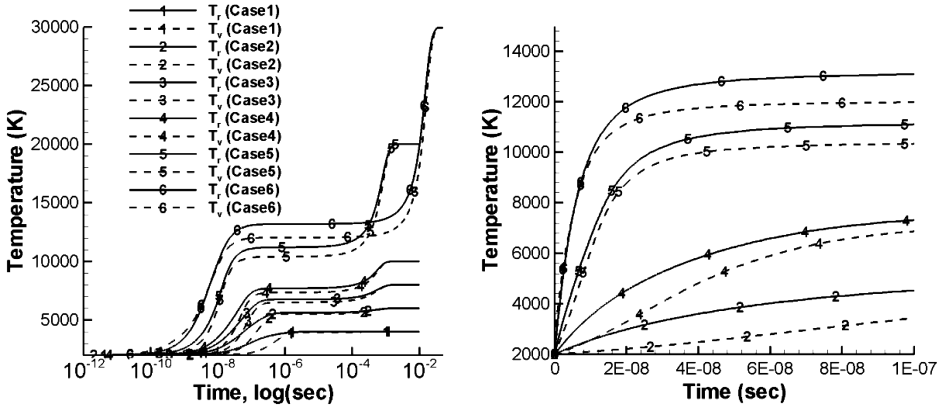

Fig. 8 Rotational and vibrational temperatures evaluated by the present master equation for heating environments: a) logarithmic time scale, and b) original time scale.

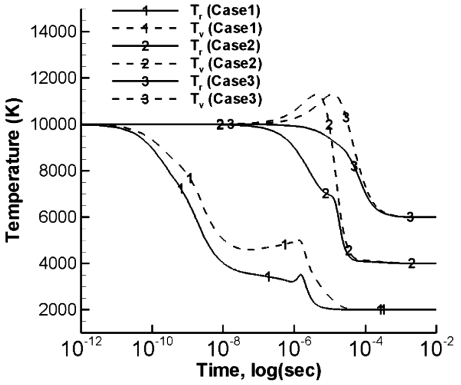

Fig. 9 Rotational and vibrational temperatures evaluated by the present master equation for cooling environments.

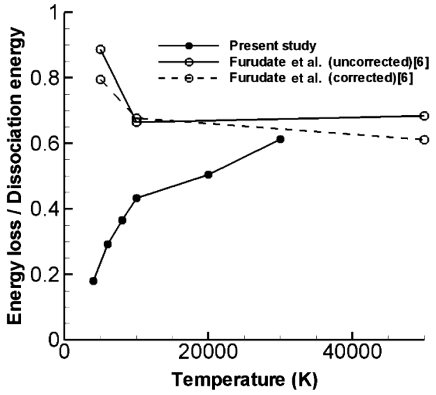

Fig. 10 Comparison of the ro-vibrational energy loss due to dissociation between the present study and Furudate et al. [6].

loss due to dissociation energy of Furudate et al. is about 0.8 or 0.9 at temperatures of 5000 K.

B. Quasi-Steady State Reaction Rate Coefficients

The QSS reaction rate coefficients [22] were derived for the reaction $M + \mathrm{H}_2(v, j) \rightarrow M + \mathrm{H} + \mathrm{H}$, where M is a H_2 populated in a Boltzmann distribution characterized by the ro-vibrational temperature. The rate of change of density of dissociated H can be written as

$$\frac{\partial N_\mathrm{H}}{\partial t} = N_{\mathrm{H}_2} N_M \iint K(v, j; c; T_\mathrm{rv}) N(v, j)\, \mathrm{d}v\, \mathrm{d}j - N_\mathrm{H} N_\mathrm{H} N_M \iint K(c; v, j; T_\mathrm{rv})\, \mathrm{d}v\, \mathrm{d}j \tag{23}$$

By using the normalized number densities, Eq. (23) can be expressed as

$$\frac{\partial N_\mathrm{H}}{\partial t} = N_{\mathrm{H}_2} N_M \iint K(v, j; c; T_\mathrm{rv}) \frac{Q_{v,j}}{Q_m} [\rho(v, j) - \rho_\mathrm{H} \rho_\mathrm{H}]\, \mathrm{d}v\, \mathrm{d}j \tag{24}$$

The normalized number density $\rho(v, j)$ is defined as $\rho_h + \rho_p \rho_\mathrm{H} \rho_\mathrm{H}$, where ρ_h and ρ_p are the homogeneous and particular solutions, respectively. Then Eq. (24) can be rewritten as

$$\frac{\partial N_\mathrm{H}}{\partial t} = N_{\mathrm{H}_2} N_M \iint K(v, j; c; T_\mathrm{rv}) \frac{Q_{v,j}}{Q_m} \rho_h\, \mathrm{d}v\, \mathrm{d}j - N_M N_\mathrm{H} N_\mathrm{H} \iint K(c; v, j; T_\mathrm{rv}) \frac{N_{\mathrm{H}_2;\mathrm{Eq}}}{N_{\mathrm{H;Eq}} N_{\mathrm{H;Eq}}} (1 - \rho_p)\, \mathrm{d}v\, \mathrm{d}j \tag{25}$$

Then the dissociation and recombination rate coefficients are determined, respectively, as

$$K_f = \iint K(v, j; c; T_\mathrm{rv}) \frac{Q_{v,j}}{Q_m} \rho_h\, \mathrm{d}v\, \mathrm{d}j \tag{26}$$

$$K_r = \iint K(v, j; c; T_\mathrm{rv}) \frac{N_{\mathrm{H}_2;\mathrm{Eq}}}{N_{\mathrm{H;Eq}} N_{\mathrm{H;Eq}}} \frac{Q_m}{Q_{v,j}} (1 - \rho_p)\, \mathrm{d}v\, \mathrm{d}j \tag{27}$$

where the state-to-state rate coefficient is the rate coefficients calculated at the ro-vibrational temperature of the QSS period. This ro-vibrational temperature can be determined from the results of the master equation study. The rate of change of density of dissociated H can be expressed with K_f and K_r as

$$\frac{\partial N_\mathrm{H}}{\partial t} = K_f(T) N_{\mathrm{H}_2} N_{\mathrm{H}_2} - K_r(T) N_\mathrm{H} N_\mathrm{H} N_{\mathrm{H}_2} \tag{28}$$

In Fig. 11, the QSS dissociation and recombination rate coefficients calculated in the present study are presented in terms of the translational temperature. For validation, the results are compared with the shock-tube experiments by Cohen and Westberg [23] for dissociation, and are also compared with the shock-tube experiments by Hurle, [24] Jacobs et al. [25], Rink [26], and Sutton, [27], and the theoretical calculations by Schwenke [5] and Furudate et al. [6] for recombination. In these calculations, the QSS dissociation and recombination rate coefficients evaluated by Eqs. (26) and (27) were used as $K_f = 5.0240 \times 10^{-6} T^{-0.88445} e^{-52530/T}$ and $K_r = 1.01975 \times 10^{-29} T^{-1.0441}$, respectively. For the dissociation rate coefficients, the experimental results are available only at the temperature range between 1000 and 5000 K. The figure shows that the present theoretical dissociation rate coefficients agree very well with the experiment. In the case of the recombination rate coefficients, the experimental results are shown to be scattered over a logarithmic range between 14.7 and 15.2 at temperatures between 3000 and

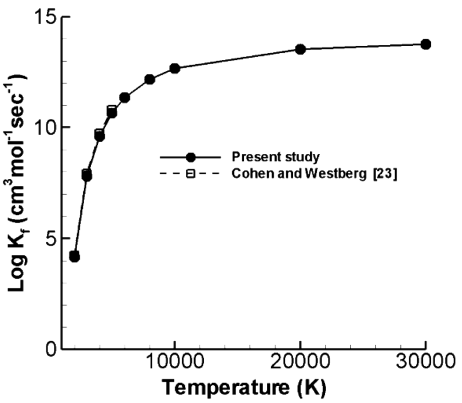

a)

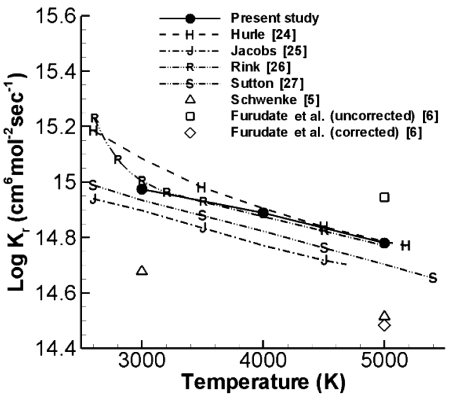

b)

Fig. 11 Comparison of reaction rate coefficients between the present study, the experiments, and other theoretical calculations: a) dissociation rate coefficients compared with the experiments by Cohen and Westberg, [23], and b) recombination rate coefficients compared with the experiments by Hurle [24], Jacobs et al. [25], Rink [26], and Sutton [27], and theoretical calculation by Schwenke [5] and Furudate et al. [6].

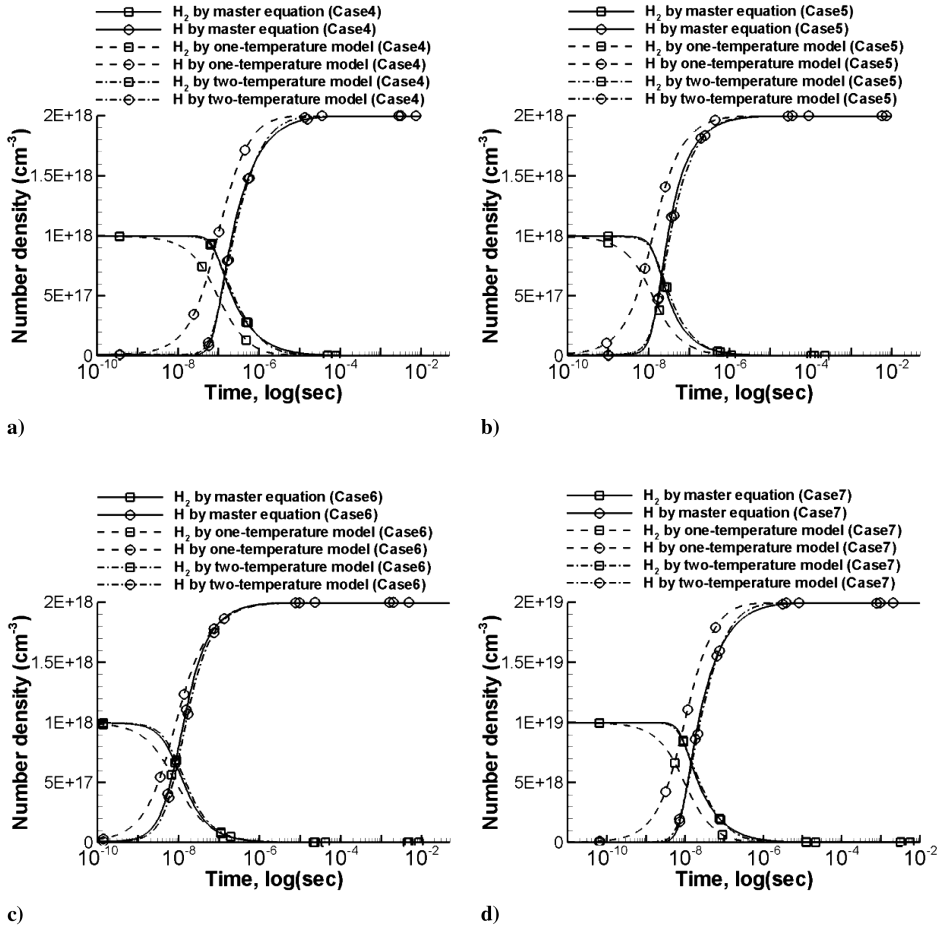

Fig. 12 Comparison of number densities of H_2 and dissociated H between the master equation study and the one-temperature and two-temperature models: a) case 4 in heating environment, b) case 5 in heating environment, c) case 6 in heating environment, and d) case 7 in heating environment.

5000 K. The theoretical recombination rate coefficients of the present study fall within this boundary. However, the theoretical calculations of Schwenke [5] and Furudate et al. [6] either overpredict or underpredict.

C. Two-Temperature Reaction Rate Coefficients

To describe nonequilibrium chemical reactions, a two-temperature model based on translational and vibrational temperatures was previously proposed by Park [22]. In the present study, the two-temperature rate expression was derived from the results of the master equation study for the $H_2 + H_2$ collisions.

First, the translational and vibrational temperatures T and T_v for the QSS period are determined from the master equation study. Also, $\partial N_H/\partial t$, N_{H_2}, and N_H are determined at the local time when the QSS condition is satisfied. $K_r(T)$ is obtained using Eq. (27), and the value of K_f is calculated using Eq. (28). Then the two-temperature rate expression is determined by curve-fitting the values of K_f and $\sqrt{TT_v}$. In this procedure, the forward rate coefficient of the two-temperature model is given as

$$K_{f\text{-two}} = 2.9674 \times 10^{-7} T_a^{-0.51649} e^{-52530/T_a} \tag{29}$$

where T_a is the geometrical mean $\sqrt{TT_v}$. In these expressions, the RVT transition effects are already accounted for, because the results of the master equation study are used in determining these parameters. Using Eq. (29), the time rate of change of N_H can be expressed as

$$\frac{\partial N_H}{\partial t} = K_{f\text{-two}}(T_a) N_{H_2} N_{H_2} - K_r(T) N_H^2 N_{H_2} \tag{30}$$

In Fig. 12, the behaviors of the number densities of H_2 and dissociated H calculated by the master equation in Eqs. (12) and (13), the one-temperature model in Eq. (28), and the two-temperature model in Eq. (30) are compared for the $H_2 + H_2$ collisions at various temperatures and number densities. Comparison of the results between the one-temperature model and the master equation study shows that the change in number density is not accurately simulated by the one-temperature model. The results of the two-temperature model are very similar to those of the master equation study for all cases. This indicates that nonequilibrium chemical reactions can be simulated more accurately by using the two-temperature model than the one-temperature model for the $H_2 + H_2$ collisions.

IV. Conclusions

The state-to-state cross sections and rates for collisional transitions of rotational and vibrational states are calculated by using quasi-classical trajectory calculations for $H_2 + H_2$ collisions. A system of master equation was constructed for a total of 348 ro-vibrational states with these rate coefficients. Unlike in existing works, the internal states of the colliding particles were assumed to be distributed under a Boltzmann distribution specified by a non-equilibrium temperature. The nonequilibrium temperature was in turn determined from the ro-vibrational energy contents. The results of present master equation calculations are different from those of Sharma [4] and of Furudate et al. [6], and agree closer with existing experimental data. From the results in heating environments, it was found that the rotational relaxation occurs faster than the vibrational relaxation at low temperatures. However, the rotational and vibrational relaxation patterns become similar for temperatures above 10,000 K. In the case of cooling environments, local increase of the rotational and vibrational temperatures was observed for $H_2 + H_2$ collisions. From the average ro-vibrational energy loss during the QSS period, it was observed that the energy loss in the present study rises with temperature. For nonequilibrium chemical

reactions, the quasi-steady-state rate coefficients and two-temperature rate coefficients were derived. From the number density relaxation, it was found that nonequilibrium chemical reactions can be simulated more accurately by using the two-temperature model than the one-temperature model for the $H_2 + H_2$ collisions.

Acknowledgment

The authors would like to acknowledge the support from the Korea Institute of Science and Technology Supercomputing Center (KSC-2008-G2-0002).

References

[1] Park, C., "Frontiers of Aerothermodynamics," NATO Research and Technology Organisation, Paper AVT-162, Sept. 2009.

[2] Mandy, M. E., and Martin, P. G., "State-to-State Rate Coefficients for $H + H_2$," *Journal of Chemical Physics*, Vol. 110, No. 16, 1999, pp. 7811–7820. doi:10.1063/1.478731

[3] Kim, J. G., Kwon, O. J., and Park, C., "Master Equation Study and Nonequilibrium Chemical Reactions for $H + H_2$ and $He + H_2$," *Journal of Thermophysics and Heat Transfer*, Vol. 23, No. 3, 2009, pp. 443–453.

[4] Sharma, S. P., "Rotational Relaxation of Molecular Hydrogen at Moderate Temperatures," *Journal of Thermophysics and Heat Transfer*, Vol. 8, No. 1, 1994, pp. 35–39. doi:10.2514/3.498

[5] Schwenke, D. W., "Calculations of Rate Constants for the Three-Body Recombination of H_2 in the Presence of H_2," *Journal of Chemical Physics*, Vol. 89, No. 4, 1988, pp. 2076–2091. doi:10.1063/1.455104

[6] Furudate, M., Fujita, K., and Abe, T., "Coupled Rotational-Vibrational Relaxation of Molecular Hydrogen at High Temperatures," *Journal of Thermophysics and Heat Transfer*, Vol. 20, No. 3, 2006, pp. 457–464. doi:10.2514/1.16323

[7] Fujita, K., and Abe, T., "Coupled Rotational-Vibrational-Dissociation Kinetics of Nitrogen Using QCT Models," AIAA, Reston, VA, Paper 2003-3779, June 2003.

[8] Lomax, H., and Steger, J. L., "Relaxation Methods in Fluid Mechanics," *Annual Review of Fluid Mechanics*, Vol. 7, No. 1, 1975, pp. 63–88. doi:10.1146/annurev.fl.07.010175.000431

[9] Eaker, C. W., "A Fast Fourier Transform Method for Quasiclassical Selection of Initial Coordinates and Momenta for Rotating Diatoms," *Journal of Chemical Physics*, Vol. 90, No. 1, 1989, pp. 105–111. doi:10.1063/1.456514

[10] Miller, W. H., *Dynamics of Molecular Collisions*, Plenum Press, New York, 1976.

[11] Bernstein, R. B., *Atom-Molecule Collision Theory-A Guide for the Eexperimentalist*, Plenum Press, New York, 1979.

[12] Mandy, M. E., Martin, P. G., and Keogh, W. J., "Why Quasiclassical Cross Sections Can Be Rotationally and Vibrationally Hot," *Journal of Chemical Physics*, Vol. 100, No. 4, 1994, pp. 2671–2676. doi:10.1063/1.466461

[13] Bartolomei, M., Hernandez, M. I., and Campos-Martinez, J., "Wave Packet Dynamics of $H_2(v_1 = 8–14) + H_2(v_2 = 0–2)$: The Role of the Potential Energy Surface on Different Reactive and Dissociative Processes," *Journal of Chemical Physics*, Vol. 122, No. 6, 2005, p. 064305. doi:10.1063/1.1846691

[14] Mandy, M. E., and Pogrebnya, S. K., "Inelastic Collisions of Molecular Hydrogen: A Comparison of Results from Quantum and Classical mechanics," *Journal of Chemical Physics*, Vol. 120, No. 12, 2004, pp. 5585–5591. doi:10.1063/1.1649722

[15] Boothroyd, A. I., Keogh, W. J., Martin, P. G., and Peterson, M. R., "An Accurate Analytic H_4 Potential energy surface," *Journal of Chemical Physics*, Vol. 116, No. 2, 2002, pp. 666–689. doi:10.1063/1.1405008

[16] Lensch, G., and Gronig, H., "Experimental Determination of Rotational Relaxation in Molecular Hydrogen and Deuterium," *Proceedings of the Eleventh International Symposium on Shock Tubes and Waves*, edited by B. Ahlborn, A. Hertzberg, and D. Russell, Univ. of Washington Press, Seattle, WA, 1977, pp. 132–139.

[17] Millikan, R. C., and White, D. R., "Systematics of Vibrational Relaxation," *Journal of Chemical Physics*, Vol. 39, No. 12, 1963, pp. 3209–3213. doi:10.1063/1.1734182

[18] Dove, J. E., and Teitelbaum, H., "The Vibrational Relaxation of H_2. I. Experimental Measurements of the Rate of Relaxation by H_2, He, Ne, Ar and Kr," *Chemical Physics*, Vol. 6, No. 3, 1974, pp. 431–444. doi:10.1016/0301-0104(74)85027-5

[19] Bray, K. N. C., "Vibrational Relaxation of Anharmonic Oscillator Molecules: Relaxation under Isothermal Oonditions," *Journal of Physics B: Atomic and Molecular Physics*, Vol. 1, No. 4, 1968, pp. 705–717. doi:10.1088/0022-3700/1/4/322

[20] McKenzie, R. L., "Diatomic Gas Dynamic Laser," *Physics of Fluids*, Vol. 15, No. 12, 1972, pp. 2163–2173. doi:10.1063/1.1693852

[21] Park, C., "Thermochemical Relaxation in Shock Tunnels," *Journal of Thermophysics and Heat Transfer*, Vol. 20, No. 4, 2006, pp. 689–698. doi:10.2514/1.22719

[22] Park, C., *Nonequilibrium Hypersonic Aerothermodynamics*, Wiley, New York, 1990.

[23] Cohen, N., and Westberg, K. R., "Chemical Kinetic Data Sheets for High-Temperature Chemical Reactions," *Journal of Physical and Chemical Reference Data*, Vol. 12, No. 3, 1983, pp. 531–590.

[24] Hurle, I. R., "Measurements of Hydrogen-Atom Recombination Rates Behind Shock Waves," *Eleventh Symposium (International) on Combustion*, Combustion Inst., Pittsburgh, PA, 1967, pp. 827–836.

[25] Jacobs, T. A., Giedt, R. R., and Cohen, N., "Kinetics of Hydrogen Halides in Shock Waves. II. New Measurement of Hydrogen Dissociation Rate," *Journal of Chemical Physics*, Vol. 47, No. 1, 1967, pp. 54–57. doi:10.1063/1.1711890

[26] Rink, J. P., "Shock Tube Determination of Dissociation Rates of Hydrogen," *Journal of Chemical Physics*, Vol. 36, No. 1, 1962, pp. 262–265. doi:10.1063/1.1732309

[27] Sutton, E. A., "Measurement of the Dissociation Rates of Hydrogen and Deuterium," *Journal of Chemical Physics*, Vol. 36, No. 11, 1962, pp. 2923–2931. doi:10.1063/1.1732403